Engineering Fracture Mechanics Vol. 31, No. 1, 119–133, 1988
Printed in Great Britain.

0013-7944/88 $3.00 + .00

STRESS CONCENTRATION OF A STRIP WITH V- OR U-SHAPED NOTCHES UNDER TRANSVERSE BENDING

NAO-AKI NODA
Mechanical Engineering Department, Kyushu Institute of Technology, Kitakyushu 804, Japan

MASA-AKI TSUBAKI
Hitachi Works, Hitachi Ltd., Hitachi 317, Japan

HIRONOBU NISITANI
Faculty of Engineering, Kyushu University, Fukuoka 812, Japan

Abstract—This paper deals with the stress concentration analyses of a 60°V-shaped single edge notch, a U-shaped single edge notch, 60°V-shaped double edge notches and U-shaped double edge notches in an infinite strip under transverse bending. The moment field induced by a moment in a semi-infinite plate is used as a fundamental solution to solve those problems. The results show that the Neuber formula gives underestimated stress concentration factors for the wide range of the notch depth. However, in the case of blunt notches, the Neuber solution of deep hyperbolic notches still gives a sufficient accuracy. The stress concentration factors of the 60°V-shaped notches and of the U-shaped notches are represented by diagrams. In addition, the stress concentration factors of a V-shaped notch in a semi-infinite plate and the effect of the notch angle on the stress concentration factor are also discussed in the appendix.

1. INTRODUCTION

THE STRESS concentration problem of a strip with double edge notches under transverse bending shown in Fig. 1 is especially important for the test specimen used in order to investigate the fatigue strength of a material. Tamate and Shioya[1] have analysed the semicircular notches and Murakami[2] has analysed the semi-elliptical notches. In this way several investigators have tried to obtain the stress concentration factors K_t of this problem. However, most of the researches on this problem have treated only a few notch sizes; therefore, the so-called Neuber's trigonometric formula eq. (1), which gives approximate values of K_t[3], has been used for more than 40 years:

$$K_{tN} = \frac{(K_{tE}-1)(K_{tH}-1)}{\sqrt{[(K_{tE}-1)^2+(K_{tH}-1)^2]}} + 1 \tag{1}$$

where K_{tE} and K_{tH} are expressed as follows.

$$\left.\begin{aligned} K_{tE} &= 1 + \frac{2(1+\nu)}{3+\nu}\sqrt{\frac{t}{\rho}} \\ K_{tH} &= \frac{2(1+\nu)\sqrt{\dfrac{w}{\rho}}}{(3+\nu)\tan^{-1}\sqrt{\dfrac{w}{\rho}} - (1-\nu)\sqrt{\dfrac{w}{\rho}}\Big/\left(\dfrac{w}{\rho}+1\right)}. \end{aligned}\right\} \tag{2}$$

This paper deals with the stress concentration problems of double V- or U-shaped edge notches in an infinitely long strip under transverse bending. The analysis is developed on the basis of the Poisson–Kirchhoff theory of thin plates[4] and by means of the body force method[5–7]. The stress concentration problems of a single V- or U-shaped notches shown in Fig. 1 are also discussed.

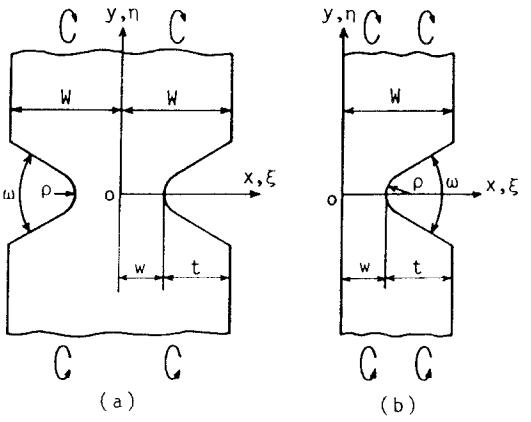

Fig. 1. (a) A double edge notched strip under transverse bending. (b) A single edge notched strip under transverse bending.

2. METHOD OF ANALYSIS

2.1. *Preliminary assumptions*

In this analysis, the deflections and stresses are found from the Poisson–Kirchhoff theory of thin plates. When the middle plane of a thin plate free from lateral load lies originally in the x–y plane, its deflection w normal to the x–y plane is governed by the biharmonic equation:

$$\nabla^4 w = 0. \tag{3}$$

The stress resultants in terms of the deflection w are expressed as follows:

$$\left.\begin{aligned} Mx &= -D\left(\frac{\partial^2 w}{\partial x^2} + \nu\frac{\partial^2 w}{\partial y^2}\right) \\ M_y &= -D\left(\frac{\partial^2 w}{\partial y^2} + \nu\frac{\partial^2 w}{\partial x^2}\right) \\ M_{xy} &= -D(1-\nu)\frac{\partial^2 w}{\partial x\,\partial y} \\ Q_x &= -D\frac{\partial}{\partial x}(\nabla^2 w) \\ Q_y &= -D\frac{\partial}{\partial y}(\nabla^2 w) \end{aligned}\right\} \tag{4}$$

where M_x, M_y are the transverse bending moments, M_{xy} is the twisting moment, and Q_x, Q_y are the transverse shearing forces, all per unit length, acting over the section $x =$ constant or $y =$ constant; ν is Poisson's ratio.

Over the free boundaries, the boundary conditions are written as follows:

$$\left.\begin{aligned} &M_n = 0, \qquad V_n = Q_n + \frac{\partial M_{nt}}{\partial s} = 0 \\ \text{or} \quad &\int_A^P V_n\,ds = \int_A^P Q_n\,ds + M_{nt}\Big|_A^P = 0 \end{aligned}\right\} \tag{5}$$

where M_n, M_{nt}, Q_n, V_n are, respectively, the bending moment, the twisting moment, the shearing force, and the equivalent shearing force, all per unit arc length of the boundary. Notation n denotes the exterior normal to the boundary, of which the arc length is s.

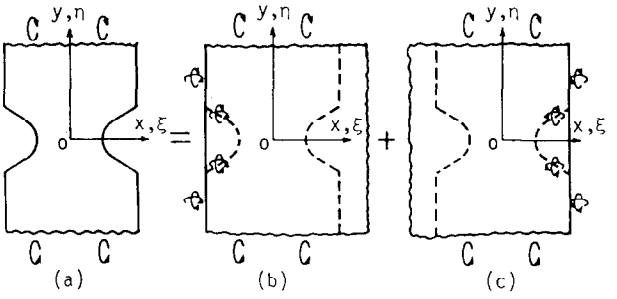

Fig. 2. Illustration of the present method of analysis for the double edge notches.

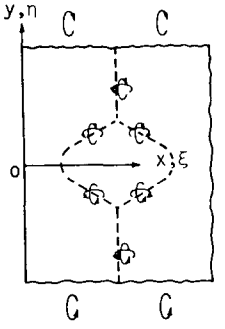

Fig. 3. Illustration of the present method of analysis for the single edge notch.

2.2. *Solution of the problem*

The body force method was originally proposed by Nisitani for solving two dimensional stress problems. In solving two dimensional problems, the stress field of a point force in an infinite plate is generally used as a fundamental solution[5]. On the other hand, in solving transverse bending problems by the body force method, the moment field induced by a moment in an infinite plate is generally used as a fundamental solution. However, in our previous paper we have proposed the analysis method using Green's function of the semi-infinite plate to solve the problem of the notched strip under tension or in-plane bending[8, 9]. Since Green's function of the semi-infinite plate is obtained in a closed form, it is convenient to use it in numerical analyses. Therefore, we are to apply the previous method to the problem of the notched strip under transverse bending.

Figure 2 shows the present method of analysis for the double edge notched strip. Consider two kinds of semi-infinite plates: one is defined in the range $-\infty < x \leqq W$ (Fig. 2a), the other in the range $-W \leqq x < \infty$ (Fig. 2b). The edges $x = 0$ and $x = W$ correspond to the stress free edges of the strip shown in Fig. 1(a). Figure 3 shows the analysis method for the single edge notched strip. As a result, the analysis method is reduced to determining the densities of the distributed moment in the semi-infinite plates shown in Figs 2 and 3.

2.3. *Definition of the densities of the distributed moment*

The densities ρ_x and ρ_y of the distributed moment in x- and y-directions are defined in eqs (6), (7):

along the notch:

$$\rho_x = \frac{\mathrm{d}M_\xi}{\mathrm{d}\eta}, \qquad \rho_y = \frac{\mathrm{d}M_\eta}{\mathrm{d}\xi} \tag{6}$$

along the strip edge:

$$\rho_x = \frac{\mathrm{d}M_\xi}{\mathrm{d}s}, \qquad \rho_y = \frac{\mathrm{d}M_\eta}{\mathrm{d}s} \tag{7}$$

where dM_ξ, dM_η denote the x- and y-component of the moment distributed along the infinitesimal arc $ds = \sqrt{[(d\xi)^2 + (d\eta)^2]}$, and (ξ, η) is a (x, y) coordinate of a point where the moment acts.

According to the definition of eq. (6), the values of ρ_x, ρ_y for the problem of an elliptical hole in an infinite plate are constant along the prospective site of the hole which must be the free edge. In this analysis, the stepped distribution (constant in each interval) of the distributed moment is substituted for the continuous varing distribution. In this procedure, the definition (6), which makes the stepped distribution approximately constant at each interval, should be used. From this viewpoint, the definition of eqs (6) and (7) is used in this analysis.

2.4. *Fundamental solution*

When a moment M_x, M_y acts at a point (ξ, η) in a semi-infinite plate, the transverse bending moments M_x, M_y, the twisting moment M_{xy} and the transverse shearing forces Q_x, Q_y are obtained as follows:

$$
\begin{aligned}
M_x^{m_x} = \frac{m_x}{2\pi}\Bigg\{ & \frac{1}{2}\Bigg[-(x-\xi)\{(1+\nu)(x-\xi)^2+(3-\nu)(y-\eta)^2\}\frac{1}{r_1^4}+(x+\xi)\{(1+\nu)(x+\xi)^2 \\
& +(3-\nu)(y-\eta)^2\}\frac{1}{r_2^4}\Bigg]+\frac{1}{(3+\nu)r_2^6}[-\{8x+(3-\nu)(3+\nu)\xi\}(y-\eta)^4 \\
& -\{4(3+\nu)(x^3+\xi^3)+6(5-\nu)(1+\nu)(x^2\xi+x\xi^2)\}(y-\eta)^2 \\
& -\{(9+4\nu+3\nu^2)x\xi+4(1+\nu)x^2+(3+\nu)(1+\nu)\xi^2\}(x+\zeta)^3]\Bigg\}
\end{aligned}
$$

$$
\begin{aligned}
M_y^{m_x} = \frac{m_x}{2\pi}\Bigg\{ & \frac{1}{2}\Bigg[-(x-\xi)\{(1+\nu)(x-\xi)^2+(-1+3\nu)(y-\eta)^2\}\frac{1}{r_1^4}+(x+\xi)\{(1+\nu)(x+\xi)^2 \\
& +(-1+3\nu)(y-\eta)^2\}\frac{1}{r_2^4}\Bigg]+\frac{1}{(3+\nu)r_2^6}[\{4(1-\nu)x+(3-\nu)(1-\nu)\xi\}(y-\eta)^4 \\
& +\{4(1-\nu)(x^3+\xi^3)+6(1-\nu^2)(x^2\xi+x\xi^2)\}(y-\eta)^2 \\
& +\{(1-\nu)(3-\nu)x\xi+(1-\nu^2)\xi^2\}(x+\xi)^3]\Bigg\}
\end{aligned}
\tag{8a}
$$

$$
\begin{aligned}
M_{xy}^{m_x} = \frac{m_x}{2\pi}\Bigg\{ & \frac{1}{2}\Bigg[(1-\nu)(y-\eta)\{(x-\xi)^2-(y-\eta)^2\}\frac{1}{r_1^4} \\
& -(1-\nu)(y-\eta)\{(x+\xi)^2-(y-\eta)^2\}\frac{1}{r_2^4}\Bigg] \\
& -\frac{(y-\eta)}{(3+\nu)r_2^6}[4(y-\eta)^4+\{4(1+\nu)(x^2+\xi^2)+2(3+6\nu-\nu^2)x\xi\}(y-\eta)^2 \\
& +\{4\nu x^2+2(3-2\nu+3\nu^2)x\xi+4\nu\xi^2\}(x+\xi)^2]\Bigg\}
\end{aligned}
$$

$$
\begin{aligned}
\int_A^P Q_n^{m_x}\,ds = \frac{m_x}{\pi}\Bigg\{ & \frac{1}{2}\Bigg[(y-\eta)\frac{1}{r_1^2}-(y-\eta)\frac{1}{r_2^2}\Bigg] \\
& -\frac{(y-\eta)}{(3+\nu)r_2^4}[-2(y-\eta)^2-\{2x^2+2(1+\nu)x\xi+2\nu\xi^2\}]\Bigg\}\Bigg|_A^P
\end{aligned}
$$

$$M_x^{m_y} = \frac{m_y}{2\pi}\left\{\frac{1}{2}\left[-(y-\eta)\{(-1+3\nu)(x-\xi)^2+(1+\nu)(y-\eta)^2\}\frac{1}{r_1^4}\right.\right.$$
$$\left.-(y-\eta)\{(-1+3\nu)(x+\xi)^2+(1+\nu)(y-\eta)^2\}\frac{1}{r_2^4}\right]$$
$$-\frac{(y-\eta)}{(3+\nu)r_2^6}[-(3+\nu)(1+\nu)(y-\eta)^4-\{4\nu(3+\nu)\xi^2$$
$$+2(1+12\nu+3\nu^2)x\xi+4(1+\nu)^2x^2\}(y-\eta)^2+\{(3+\nu)(1-3\nu)\xi^2$$
$$\left.-4(1+3\nu^2)\xi x-(1+3\nu)(1+\nu)x^2\}(x+\xi)^2]\right\}$$

$$M_y^{m_y} = \frac{m_y}{2\pi}\left\{\frac{1}{2}\left[-(y-\eta)\{(3-\nu)(x-\xi)^2+(1+\nu)(y-\eta)^2\}\frac{1}{r_1^4}\right.\right.$$
$$\left.-(y-\eta)\{(3-\nu)(x+\xi)^2+(1+\nu)(y-\eta)^2\}\frac{1}{r_2^4}\right]-\frac{y-\eta}{(3+\nu)r_2^6}[(1-\nu^2)(y-\eta)^4$$
$$-\{-4\nu(1-\nu)\xi^2+2(1-3\nu)(1-\nu)\xi x\}(y-\eta)^2$$
$$\left.-\{(1-3\nu)(1-\nu)\xi^2-4(1-\nu)^2x\xi+(1-\nu^2)x^2\}(x+\xi)^2]\right\}$$

$$M_{xy}^{m_y} = \frac{m_y}{2\pi}\left\{\frac{1}{2}\left[(1-\nu)(x-\xi)\{(y-\eta)^2-(x-\xi)^2\}\frac{1}{r_1^4}+(1-\nu)(x+\xi)\{(y-\eta)^2-(x+\xi)^2\}\frac{1}{r_2^4}\right]\right.$$
$$+\frac{1}{(3+\nu)r_2^6}[-\{(3-\nu)(1+\nu)x+4\xi\}(y-\eta)^4$$
$$-\{4(1+\nu)(x^3+\xi^3)+6(1+4\nu-\nu^2)(x^2\xi+\xi^2x)\}(y-\eta)^2$$
$$\left.-\{(1+\nu)^2x^2+(3+2\nu+3\nu^2)x\xi+4\nu\xi^2\}(x+\xi)^3]\right\}$$

$$\int_A^P Q_n^{m_y}\,ds = \frac{m_y}{\pi}\left\{\frac{1}{2}\left[-(x-\xi)\frac{1}{r_1^2}-(x+\xi)\frac{1}{r_2^2}\right]\right.$$
$$\left.+\frac{1}{(3+\nu)r_2^4}[\{(1+\nu)x+2\xi\}(y-\eta)^2+\{(1+\nu)x+2\nu\xi\}(x+\xi)^2]\right\}\Bigg|_A^P \qquad (8b)$$

where $r_1^2=(x-\xi)^2+(y-\eta)^2$, $r_2^2=(x+\xi)^2+(y-\eta)^2$.

3. RESULTS AND DISCUSSION

In the following discussion, we use the stress concentration factors SCFs based on the net section width w^*.

$$K_t=\frac{\sigma_{max}}{\sigma_n}, \qquad \sigma_n=\frac{6M}{w^*h^2} \qquad (9)$$

where $w^*=2w$ for the double notches shown in Fig. 1(a) and $w^*=w$ for the single edge notch shown in Fig. 1(b). In eq. (9), σ_{max} is the maximum stress at the root of the notch, σ_n is the nominal stress, h is the plate thickness and M is the external bending moment. Poisson's ratio is assumed to be 0.3 in this analysis.

3.1. *SCFs of the semicircular notch*

Table 1 shows SCFs of the present analysis for the semicircular notch. The results of Tamate–Shioya[1] and Neuber[3] are also shown. It is found that the SCFs of the double notches have a close agreement with the single notch. The results in Table 1 are plotted in Fig. 4.

Table 1. SCFs of the semicircular notches

ρ/W	Present analysis (Double)	Present analysis (Single)	Tamate (Double)	Neuber
0.02	1.756	1.756		1.76
0.03	1.739	1.739		1.75
0.05	1.706	1.706		1.71
0.1	1.626	1.627	1.625	1.62
0.2	1.486	1.488	1.485	1.45
0.3	1.366	1.371	1.366	1.32
0.4	1.266	1.274		1.22
0.5	1.184	1.195		1.16
0.6	1.120	1.133		1.11
0.7	1.072	1.086		1.07
0.8	1.039	1.050		1.04
0.9	1.017	1.022		1.02

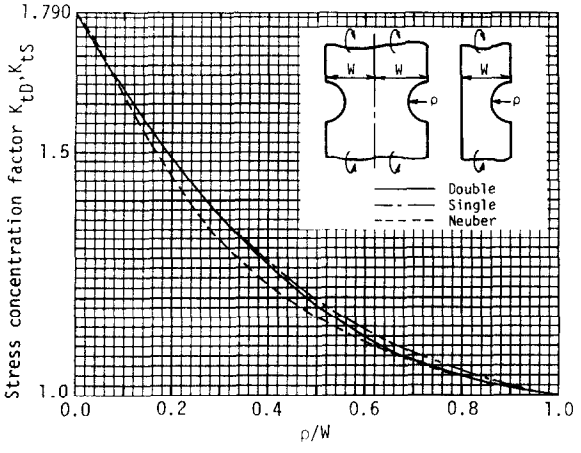

Fig. 4. SCFs of the semicircular notches.

3.2. *SCFs of the partially-circular notch*

In Table 2, SCFs of partially-circular notches in a strip are shown. These specimens are frequently used for fatigue tests of metals. The values due to the Neuber formula K_{tN} and the valucs of deep hyperbolic notches K_{tH} are also shown to be compared with the value of the present analysis. It is found that the solution of deep hyperbolic notch[3] gives a sufficient accuracy for blunt notches.

Table 2. SCFs of the partially-circular notches

W/w	1.1		1.2		1.5		2.0		∞
ρ/w	K_t	K_{tN}	K_t	K_{tN}	K_t	K_{tN}	K_t	K_{tN}	K_{tH}
1.0	1.082	1.073	1.089	1.077	1.091	1.079	1.089	1.080	1.081
2.0	1.045	1.038	1.046	1.039	1.044	1.040	1.042	1.040	1.040
5.0	1.018	1.015	1.017	1.016	1.016	1.016	1.015	1.016	1.016
10.0	1.009	1.008	1.008	1.008	1.008	1.008	1.008	1.008	1.008

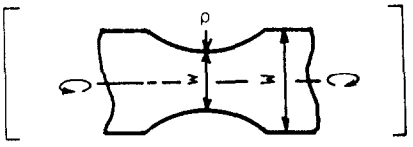

Table 3. SCFs of the 60°V-shaped notches

	ρ/W=0.02			ρ/W=0.03			ρ/W=0.05			ρ/W=0.1		
t/W	K_{tD}	K_{tS}	K_{tN}	K_{tD}	K_{tS}	K_{tN}	K_{tD}	K_{tS}	K_{tN}	K_{tD}	K_{tS}	K_{tN}
0.02	1.752	1.752	1.76	1.599	1.599	1.62	1.450	1.450	1.48	1.306	1.306	1.33
0.05	2.181	2.181	2.14	1.941	1.942	1.93	1.702	1.702	1.71	1.467	1.467	1.49
0.1	2.582	2.583	2.49	2.267	2.268	2.20	1.946	1.947	1.91	1.623	1.624	1.62
0.2	2.956	2.959	2.80	2.573	2.575	2.44	2.177	2.179	2.07	1.770	1.772	1.71
0.3	3.073	3.080	2.89	2.667	2.673	2.50	2.245	2.251	2.10	1.808	1.813	1.71
0.4	3.053	3.064	2.86	2.647	2.656	2.46	2.224	2.233	2.07	1.785	1.794	1.67
0.5	2.942	2.957	2.75	2.550	2.564	2.37	2.143	2.156	1.98	1.722	1.733	1.61
0.6	2.759	2.779	2.58	2.394	2.412	2.22	2.016	2.032	1.87	1.626	1.641	1.52
0.7	2.512	2.535	2.35	2.184	2.206	2.03	1.847	1.867	1.72	1.504	1.522	1.42
0.8	2.188	2.215	2.05	1.913	1.937	1.79	1.632	1.655	1.53	1.356	1.377	1.30
0.9	1.745	1.772	1.64	1.547	1.572	1.46	1.353	1.377	1.30	1.178	1.200	1.16

	ρ/W=0.2			ρ/W=0.5			ρ/W=1.0		
t/W	K_{tD}	K_{tS}	K_{tN}	K_{tD}	K_{tS}	K_{tN}	K_{tD}	K_{tS}	K_{tN}
0.02	1.208	1.208	1.23	1.123	1.123	1.14	1.082	1.082	1.09
0.05	1.309	1.310	1.33	1.176	1.177	1.19	1.112	1.113	1.12
0.1	1.402	1.403	1.41	1.218	1.219	1.22	1.132	1.134	1.12
0.2	1.483	1.486	1.45	1.245	1.248	1.22	1.138	1.142	1.12
0.3	1.498	1.503	1.43	1.239	1.245	1.21	1.127	1.133	1.11
0.4	1.474	1.482	1.40	1.216	1.225	1.18	1.109	1.118	1.10
0.5	1.424	1.435	1.35	1.184	1.195	1.16	1.089	1.100	1.08
0.6	1.356	1.370	1.30	1.145	1.159	1.13	1.068	1.080	1.06
0.7	1.273	1.291	1.23	1.105	1.120	1.10	1.048	1.060	1.05
0.8	1.180	1.199	1.16	1.065	1.080	1.06	1.031	1.040	1.03
0.9	1.082	1.100	1.08	1.030	1.040	1.03	1.015	1.020	1.02

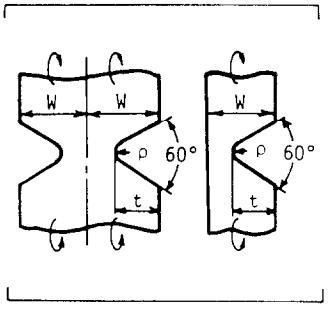

3.3. *SCFs of the 60° V-shaped notch*

Table 3 shows SCFs of the double 60°V-shaped notch K_{tD} and of the single 60°V-shaped notch K_{tS}. In the case of the shallow notch ($t < \rho/2$), those values express SCFs of the partially-circular notch. Neuber's values K_{tN} given by eq. (1) are also shown. The results in Table 3 are plotted in Figs 5 and 6 so as to be useful further in design or research.

In Fig. 5, the ordinate represents the values of SCFs and the abscissa represents the relative notch depth t/W. After comparing the value, we conclude that Neuber's rule eq. (1) underestimates SCFs of the 60°V-shaped notch by about 7% for the worst case. The charts of SCFs are also shown in different ways from Fig. 6. In Fig. 6, the abscissa represents the relative notch radius ρ/W. Using Figs 5 and 6, the SCF not calculated in this paper can be estimated.

3.4. *SCFs of the U-shaped notch*

Table 4 shows SCFs of the double U-shaped notch K_{tD} and of the single U-shaped notch K_{ts}. The results in Table 4 are plotted in Figs 7 and 8 so as to be useful further in design or research. Neuber's rule eq. (1) underestimates SCFs of the U-shaped notch by about 18% for the worst case. The difference between U-shape and V-shape increases when relative notch radius ρ/W decreases.

3.5. *Special relationship between the notch shape and the SCF*

Tables 5–8 show the values K_t/K_{to}, where K_t means the SCF of the U- or V-notch in the strip and K_{to} means the SCF of the U- or V-shaped notch in the semi-infinite plate (see appendix). In Tables 5–8, it is found that the values K_t/K_{to} are mainly determined by the relative notch depth t/W alone, especially for the shallow notches. Utilizing this fact, we can estimate the SCF of sharp U- or V-notched strip not calculated in this paper ($\rho/W < 0.02$) from the SCF of the U- or V-shaped semi-infinite plate. The procedure is summarized as follows.

Step 1. Obtain the SCF K_{to} of the given U- or V-notch in the semi-infinite plate using the results shown in the appendix.

Step 2. The value K_t/K_{to} is obtained from the value t/W by using Tables 5–8.

Step 3. The SCF of the given U- or V-shaped notch in the strip is given by the equation: $K_t = K_{to}(K_t/K_{to})$.

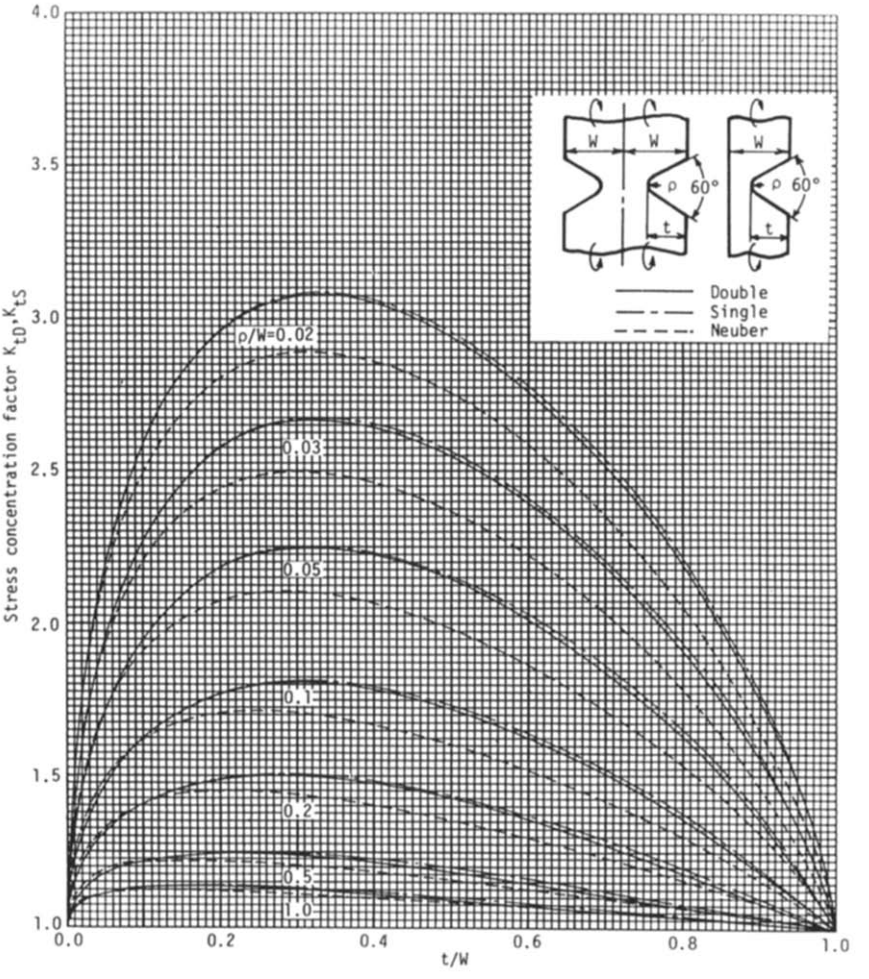

Fig. 5. SCFs of the 60°V-shaped notches.

Table 4. SCFs of the U-shaped notches

	ρ/W=0.02			ρ/W=0.03			ρ/W=0.05			ρ/W=0.1		
t/W	K_{tD}	K_{tS}	K_{tN}	K_{tD}	K_{tS}	K_{tN}	K_{tD}	K_{tS}	K_{tN}	K_{tD}	K_{tS}	K_{tN}
0.02	1.756	1.756	1.76	1.599	1.599	1.62	1.450	1.450	1.48	1.306	1.306	1.33
0.05	2.210	2.210	2.14	1.951	1.952	1.93	1.706	1.706	1.71	1.467	1.467	1.49
0.1	2.686	2.687	2.49	2.318	2.319	2.20	1.962	1.963	1.91	1.626	1.627	1.62
0.2	3.201	3.203	2.80	2.714	2.716	2.44	2.239	2.241	2.07	1.783	1.786	1.71
0.3	3.419	3.424	2.89	2.879	2.884	2.50	2.348	2.353	2.10	1.838	1.842	1.71
0.4	3.457	3.465	2.86	2.900	2.909	2.46	2.354	2.362	2.07	1.827	1.834	1.67
0.5	3.362	3.374	2.75	2.817	2.827	2.37	2.282	2.293	1.98	1.768	1.778	1.61
0.6	3.156	3.171	2.58	2.646	2.661	2.22	2.147	2.162	1.87	1.670	1.683	1.52
0.7	2.847	2.867	2.35	2.394	2.412	2.03	1.953	1.971	1.72	1.537	1.554	1.42
0.8	2.424	2.447	2.05	2.054	2.076	1.79	1.699	1.720	1.53	1.373	1.393	1.30
0.9	1.847	1.874	1.64	1.600	1.625	1.46	1.373	1.396	1.30	1.180	1.202	1.16

	ρ/W=0.2			ρ/W=0.5			ρ/W=1.0		
t/W	K_{tD}	K_{tS}	K_{tN}	K_{tD}	K_{tS}	K_{tN}	K_{tD}	K_{tS}	K_{tN}
0.02	1.208	1.208	1.23	1.123	1.123	1.14	1.082	1.082	1.09
0.05	1.309	1.310	1.33	1.176	1.177	1.19	1.112	1.113	1.12
0.1	1.402	1.403	1.41	1.218	1.219	1.22	1.132	1.134	1.12
0.2	1.486	1.488	1.45	1.245	1.248	1.22	1.138	1.142	1.12
0.3	1.502	1.507	1.43	1.239	1.245	1.21	1.127	1.133	1.11
0.4	1.481	1.489	1.40	1.216	1.225	1.18	1.109	1.118	1.10
0.5	1.434	1.445	1.35	1.184	1.195	1.16	1.089	1.100	1.08
0.6	1.365	1.379	1.30	1.146	1.159	1.13	1.068	1.080	1.06
0.7	1.279	1.296	1.23	1.105	1.120	1.10	1.048	1.060	1.05
0.8	1.182	1.201	1.16	1.065	1.080	1.06	1.030	1.040	1.03
0.9	1.082	1.100	1.08	1.030	1.040	1.03	1.015	1.020	1.02

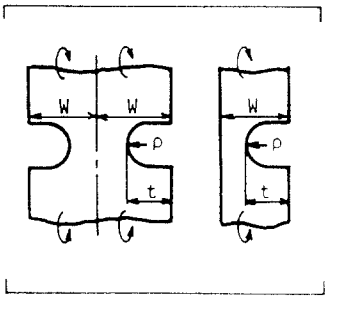

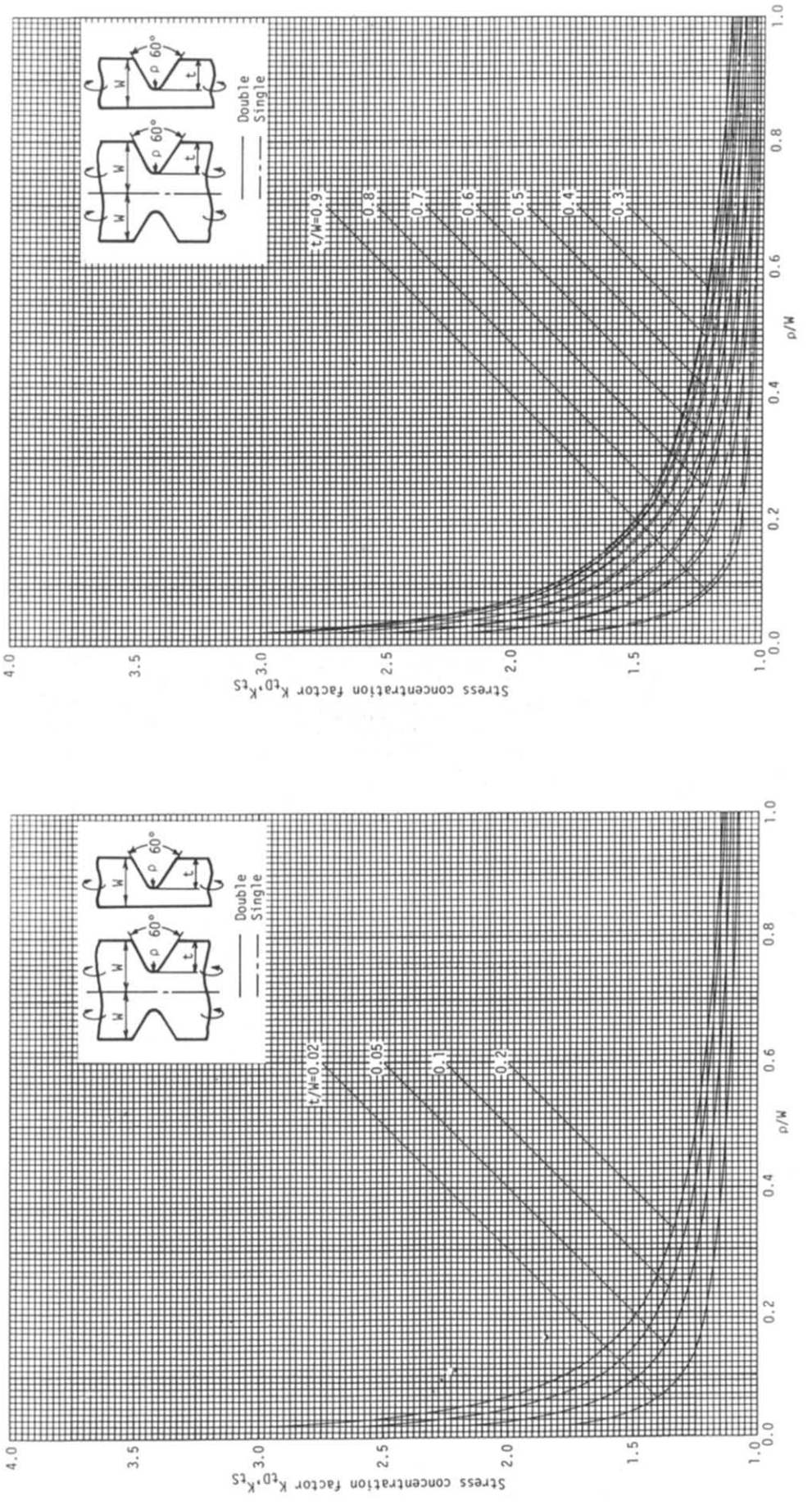

Fig. 6. SCFs of the 60°V-shaped notches.

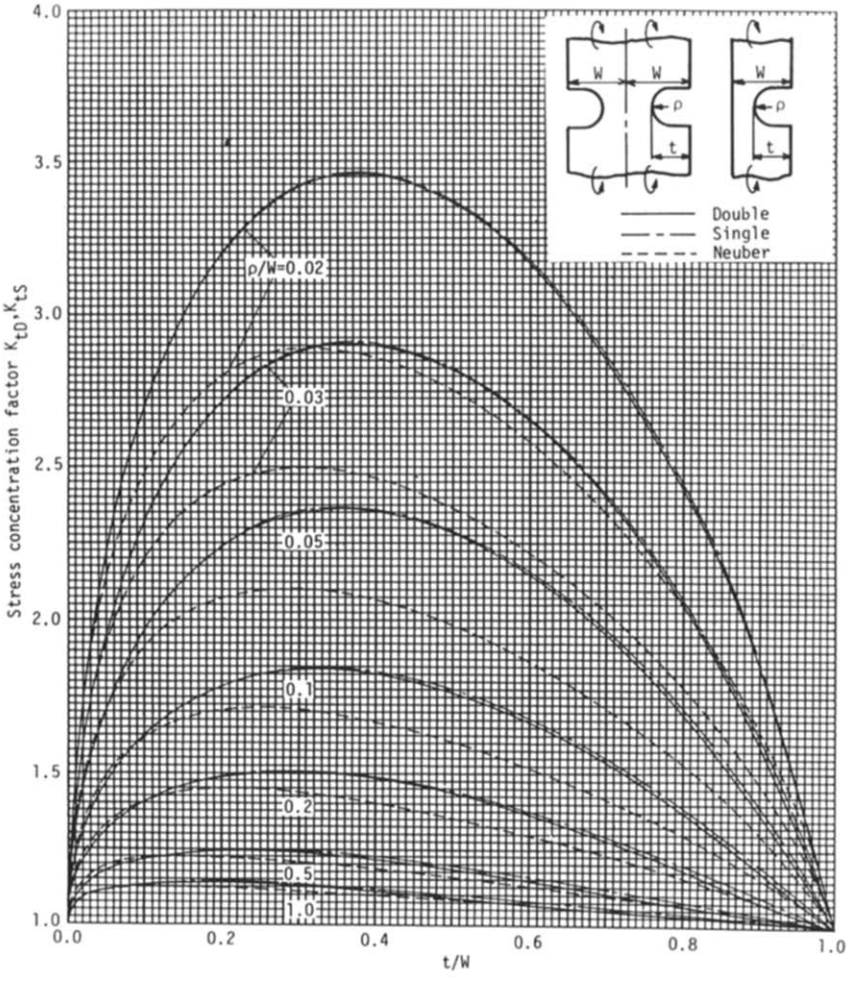

Fig. 7. SCFs of the U-shaped notches.

Table 5. Values of $K_t/K_t|_{t/W\to 0}$ of the 60°V-shaped double notches

ρ/W / t/W	0.02	0.03	0.05	0.1	0.2	0.5	1.0
0.02	0.980	0.981	0.980	0.980	0.981	0.981	0.982
0.05	0.952	0.953	0.952	0.953	0.953	0.955	0.957
0.1	0.906	0.906	0.906	0.908	0.910	0.914	0.919
0.2	0.819	0.820	0.821	0.824	0.829	0.842	0.854
0.3	0.737	0.738	0.741	0.747	0.756	0.776	0.798
0.4	0.661	0.663	0.666	0.673	0.687	0.717	0.750
0.5	0.587	0.589	0.594	0.604	0.622	0.662	0.707
0.6	0.515	0.518	0.524	0.537	0.560	0.613	0.669
0.7	0.443	0.447	0.454	0.471	0.501	0.568	0.636
0.8	0.368	0.373	0.383	0.406	0.445	0.529	0.608
0.9	0.280	0.289	0.304	0.338	0.393	0.494	0.583

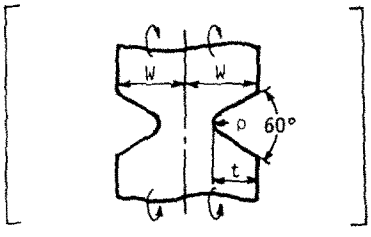

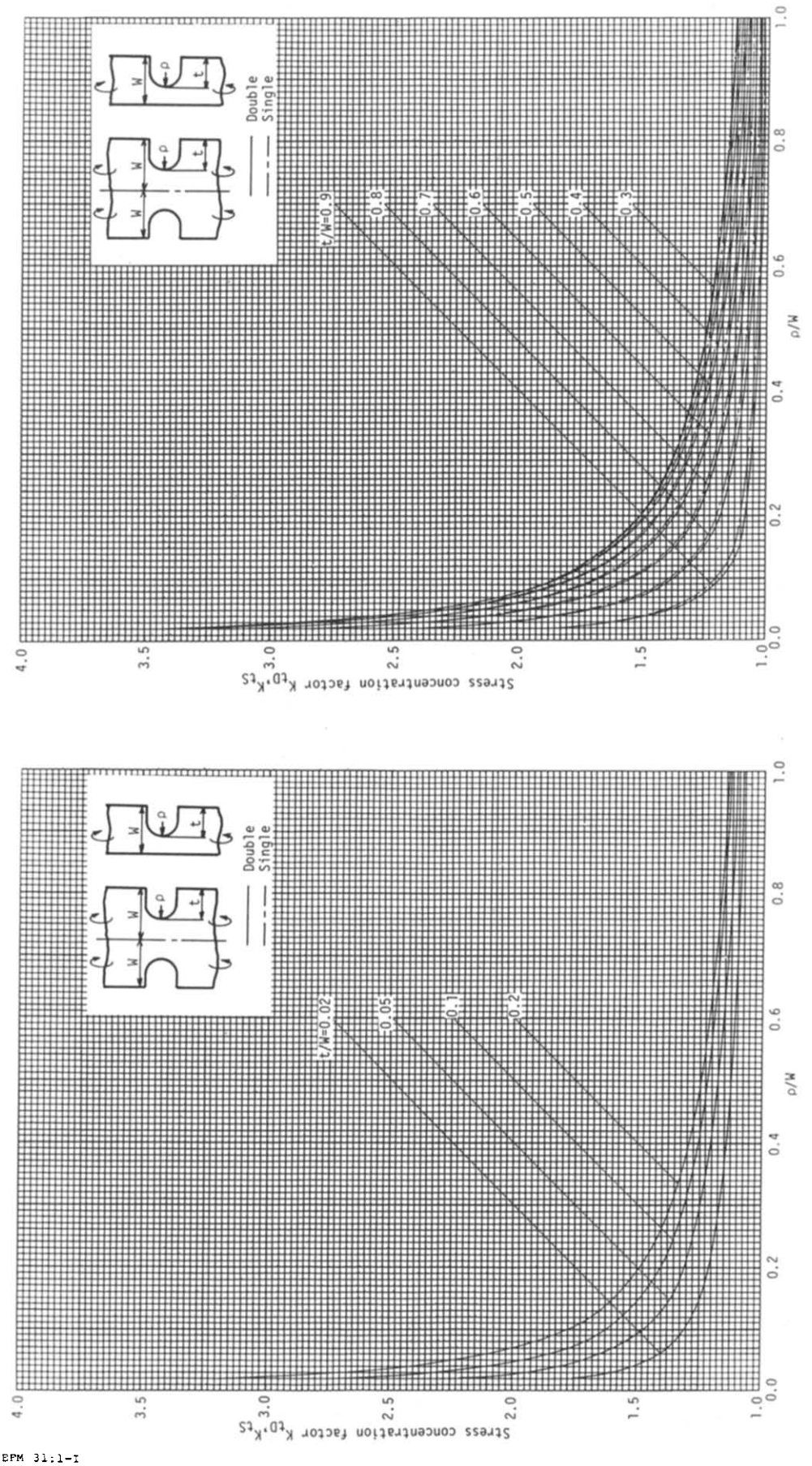

Fig. 8. SCFs of the U-shaped notches.

Table 6. Values of $K_t/K_t|_{t/W\to 0}$ of the 60°V-shaped single notch

ρ/W / t/W	0.02	0.03	0.05	0.1	0.2	0.5	1.0
0.02	0.980	0.981	0.980	0.980	0.981	0.981	0.982
0.05	0.952	0.953	0.952	0.953	0.953	0.955	0.958
0.1	0.906	0.906	0.907	0.908	0.911	0.915	0.920
0.2	0.820	0.820	0.822	0.825	0.831	0.844	0.857
0.3	0.739	0.740	0.743	0.749	0.759	0.780	0.802
0.4	0.663	0.665	0.668	0.676	0.690	0.722	0.756
0.5	0.590	0.593	0.597	0.608	0.626	0.668	0.714
0.6	0.519	0.522	0.528	0.542	0.566	0.620	0.677
0.7	0.447	0.452	0.459	0.477	0.508	0.576	0.644
0.8	0.372	0.378	0.388	0.412	0.452	0.536	0.613
0.9	0.285	0.293	0.310	0.345	0.399	0.499	0.586

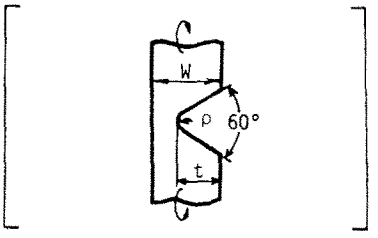

Table 7. Values of $K_t/K_t|_{t/W\to 0}$ of the U-shaped double notches

ρ/W / t/W	0.02	0.03	0.05	0.1	0.2	0.5	1.0
0.02	0.981	0.981	0.980	0.980	0.981	0.981	0.982
0.05	0.953	0.953	0.953	0.953	0.953	0.955	0.957
0.1	0.906	0.906	0.906	0.908	0.910	0.914	0.919
0.2	0.817	0.817	0.819	0.824	0.830	0.842	0.854
0.3	0.733	0.734	0.737	0.744	0.757	0.776	0.798
0.4	0.651	0.654	0.659	0.668	0.684	0.716	0.750
0.5	0.573	0.576	0.582	0.595	0.618	0.661	0.707
0.6	0.494	0.499	0.507	0.524	0.553	0.613	0.669
0.7	0.415	0.421	0.431	0.453	0.491	0.567	0.636
0.8	0.332	0.340	0.354	0.384	0.432	0.526	0.607
0.9	0.239	0.250	0.271	0.314	0.379	0.492	0.582

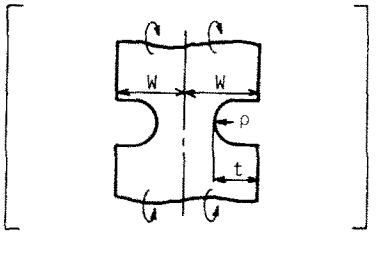

4. CONCLUSION

In this paper, the stress concentration problems of the single edge notched strip and of the double edge notched strip under transverse bending have been considered. Green's function of the semi-infinite plate in the closed form was used as a fundamental solution for those problems. The conclusions can be made as follows:

(1) The stress concentration factors K_t of the 60° V-shaped notch and of the U-shaped notch are systematically calculated under various geometrical conditions. The Neuber formula is found to give an underestimated stress concentration factor for the 60° V-shaped notch by about 7% and for the U-shaped notch by about 18%. The stress concentration factors are illustrated in the diagrams for design and research.

Table 8. Values of $K_t/K_t|_{t/W\to 0}$ of the U-shaped single notch

t/W \ ρ/W	0.02	0.03	0.05	0.1	0.2	0.5	1.0
0.02	0.981	0.981	0.980	0.980	0.981	0.981	0.982
0.05	0.953	0.954	0.953	0.953	0.953	0.955	0.958
0.1	0.906	0.906	0.907	0.908	0.911	0.915	0.920
0.2	0.817	0.818	0.820	0.825	0.831	0.844	0.857
0.3	0.734	0.736	0.738	0.746	0.759	0.780	0.802
0.4	0.653	0.656	0.661	0.671	0.688	0.721	0.756
0.5	0.575	0.578	0.585	0.599	0.622	0.667	0.714
0.6	0.496	0.501	0.510	0.528	0.558	0.620	0.677
0.7	0.418	0.424	0.435	0.458	0.498	0.575	0.644
0.8	0.335	0.343	0.358	0.390	0.439	0.534	0.613
0.9	0.243	0.254	0.276	0.320	0.385	0.497	0.585

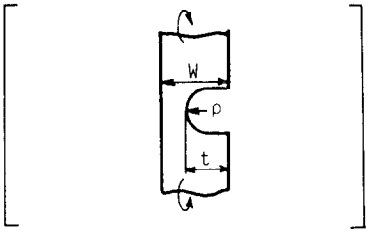

(2) In the transverse bending problem of the strip, the stress concentration factors of the single edge notch and of the double edge notches are in close agreement except for the case of the deep notch.

(3) The stress concentration factors of the partially-circular notch for fatigue test specimens can be estimated accurately by Neuber's solution of deep hyperbolic notch.

(4) The values K_t/K_{to} ($K_{to} = K_t|_{t/W\to 0}$) are found to be mainly determined by the relative notch depth t/W alone. Taking this into account, the values of the extremely sharp notch in the strip not calculated in this paper can also be estimated from the values of K_{to}.

REFERENCES

[1] O. Tamate and S. Shioya, On the transverse flexure of an infinite strip with semicircular notches on both edges. *Trans. Japan Soc. Mech. Engrs* **24**, 809–818 (1958).
[2] Y. Murakami and S. Araki, Application of the body force method to the calculation of the stress concentration factor for an elliptical hole or an elliptical-arc notch in the plate under transverse bending. *Trans. Japan Soc. Mech. Engrs* **45**, 998–1006 (1979).
[3] H. Neuber, *Kerbspannungslehre* (2nd edn). Springer, Berlin (1958).
[4] S. P. Timoshenko and S. W. Krieger, *Theory of Plates and Shells* (2nd edn), p. 326. McGraw-Hill, New York (1959).
[5] H. Nisitani, Two-dimensional stress problem solved using an electric digital computer. *J. Japan Soc. Mech. Engrs* **70**, 627–632 (1967) [*Bull. Japan Soc. Mech. Engrs* **11**, 14–23 (1968)].
[6] H. Nisitani, *Solution of notch problems by body force method. Stress Analysis of Notched Problems* (Edited by G. C. Sih), pp. 1–68, Noordhoff, Leyden (1978).
[7] H. Nisitani and N.-A. Noda, Stress concentration of a cylindrical bar with a V-shaped circumferential groove under torsion, tension or bending. *Engng Fracture Mech.* **20**, 743–766 (1984).
[8] H. Nisitani and N.-A. Noda, Stress concentration of a strip with double edge notches under tension or in-plane bending. *Engng Fracture Mech.* **23**, 1051–1065 (1986).
[9] N.-A. Noda and H. Nisitani, Stress concentration of a strip with a single edge notch. *Engng Fracture Mech.* **28**, 223–238 (1987).

APPENDIX

1. *SCFs of a 60° V-shaped notch and of a U-shaped notch in a semi-infinite plate*

Stress concentration factors of a V- or U-shaped notch in a semi-infinite plate can also be calculated by the body force method. These values are utilized for estimating the SCFs of the sharp notch in a strip from the previous discussion in Section 3.5. In Table A1, the SCFs of the 60°V-shaped notch K_{tv} and of the U-shaped notch K_{tu} in the semi-infinite plate are shown for the wide range of t/ρ. The SCFs of a semi-elliptical notch K_{te} and of an elliptical hole K_{th} are also shown.

The ratios K_{tv}/K_{th} and K_{te}/K_{th} are plotted in Fig. A1, where the abscissa represents $\sqrt{(t/\rho)}$. Using Fig. A1, we can estimate the SCFs of a 60°V-shaped notch and of a U-shaped notch for the wide range of $\sqrt{(t/\rho)}$.

Table A1. SCFs of a 60°V-shaped notch and of a U-shaped notch in a semi-infinite plate

t/ρ	$\sqrt{t/\rho}$	K_{tv}	K_{tu}	K_{te}	K_{th}
0.0625	0.25	1.182	1.182	1.197	1.197
0.25	0.5	1.374	1.374	1.395	1.394
1	1	1.788	1.790	1.790	1.788
2	1.414	2.147	2.165	2.119	2.114
4	2	2.652	2.733	2.584	2.576
8	2.828	3.343	3.574	3.241	3.228
16	4	4.267	4.804	4.170	4.152
32	5.657	5.488	6.586	5.482	5.457
64	8	7.091	9.14	7.340	7.303
100	10	8.38	11.3	8.924	8.879
225	15	11.4	16.7	12.88	12.82

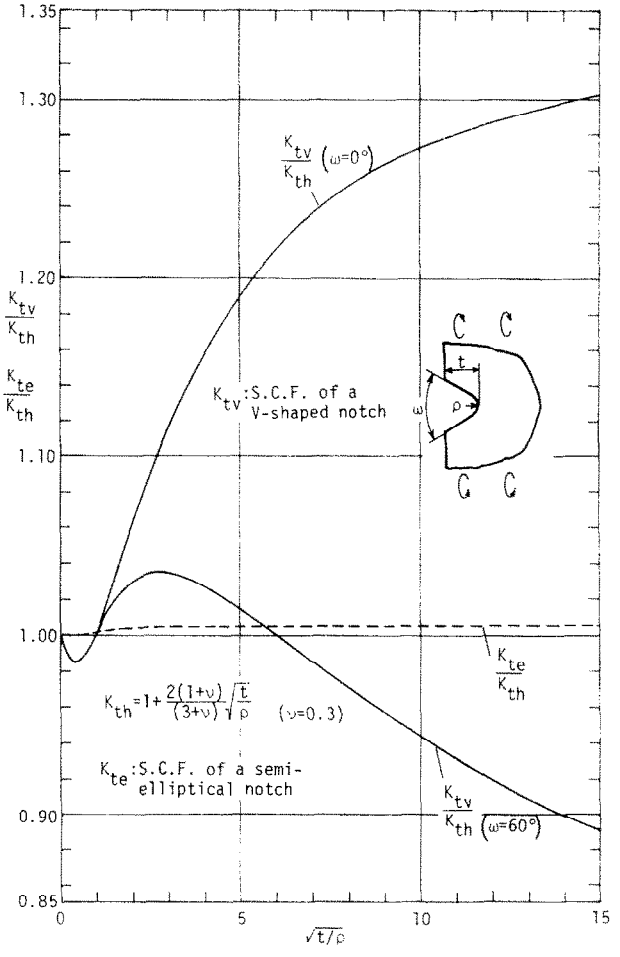

Fig. A1. Values K_{tv}/K_{th} and K_{te}/K_{th}.

Table A2. Effect of the notch angle ω on the SCF

deg / t/ρ	0	30	60	90	120	150
1	1.790	1.789	1.788	1.777	1.729	1.559
2	2.165	2.161	2.147	2.102	1.978	1.688
4	2.732	2.708	2.652	2.528	2.279	1.829
8	3.574	3.494	3.343	3.073	2.635	1.982

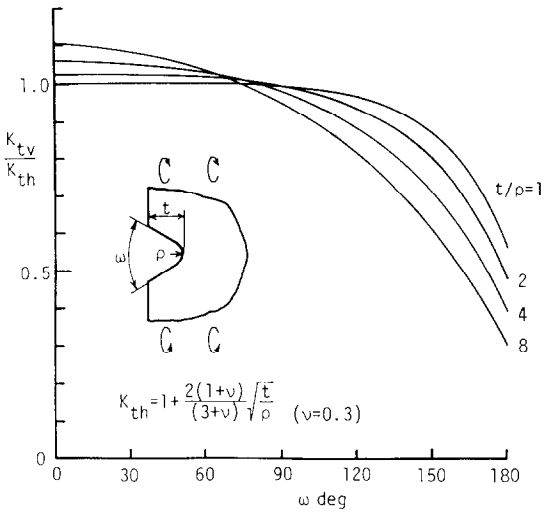

Fig. A2. Effect of the notch angle ω on the SCF.

2. *Effect of the notch angle on the SCF*

Table A2 shows SCFs of the *V*-shaped notch with the notch angle ω in the semi-infinite plate. The results of Table A2 are plotted in Fig. A2. Compared with the two dimensional problem[6], the effect of the notch angle on the SCF is larger; thus in the transverse bending problem the stress concentration can be more reduced by increasing the notch angle, especially for the sharp notch.

(*Received* 16 *June* 1987)